

INTERNATIONAL COLLABORATION ON ADVANCED NEUTRON SOURCES

22-26 September, 1986

Liquid and Amorphous Total Scattering Instrument at KENS

- HIT -

M. Misawa, T. Fukunaga<sup>\*</sup>, T. Yamaguchi<sup>\*\*</sup> and N. Watanabe

National Laboratory for High Energy Physics,  
Oho-machi, Tsukuba-gun, Ibaraki-ken, 305, Japan

\* Research Institute for Iron, Steel and Other Metals,  
Tohoku University, Sendai 980, Japan

\*\* Department of Electronic Chemistry,  
Tokyo Institute of Technology,  
Nagatuta, Midori-ku, Yokohama 227, Japan

Abstract

Liquid and Amorphous Total Scattering Instrument (HIT) at KENS is in operation since 1980. It was originally designed to measure the  $S(Q)$  of liquids and amorphous solids composed of heavy nuclei with high count rate and modest resolution of the momentum transfer  $Q$ . Recently proposals which desire to measure the  $S(Q)$  of materials composed of light nuclei or with better resolution are increasing in number. The effects of the resolution and the inelastic scattering on observed  $S(Q)$  are, therefore, reexamined using machine parameters of the HIT. Current performance of the HIT is briefly reported as well.

## 1. Introduction

The Liquid and Amorphous Total Scattering Instrument (HIT) at KENS was constructed in 1980. Since then it has been operated for more than 5 years. During this period many users from outside universities performed measurements of  $S(Q)$  on various kinds of liquids and amorphous materials. Many scientific results have been obtained using this machine and significant contributions to the structure determination of liquids and amorphous solids have been made.

The HIT machine was originally designed to measure the  $S(Q)$  of liquids and amorphous solids with high count rates and modest resolution of momentum transfer  $Q$ .<sup>1)</sup> The target materials we supposed were those composed of heavy nuclei or those of which inelastic scattering is not significant.

Recently proposals to measure the  $S(Q)$  for the materials containing light nuclei or with better resolution are increasing in number at KENS. Therefore we reexamined the effects of the resolution and the inelastic scattering on observed  $S(Q)$  using the machine parameters of the HIT. In this report we summarize the current performance of the HIT machine briefly and discuss how the resolution and the inelastic scattering affect the observed  $S(Q)$ .

## 2. Outline of the machine

A schematic drawing of the current HIT machine is shown in Fig. 1. The machine views the ambient temperature solid polyethylene moderator. A sample is located 5,053 mm from the moderator. The evacuated sample chamber is 450 mm in diameter so that it has enough room to install a sample changer and sample environmental equipments such as a high temperature furnace, low temperature refrigerator, magnet and so on. The neutron flux at the sample position is about  $5 \times 10^5$  n/cm<sup>2</sup>/sec/2 $\mu$ A in the range of 0.3 to 0.7 Å which we use mainly for  $S(Q)$  measurement.

The neutron detectors used are He-3 gas counters (1/2" in diameter, 12" in active length and 20 atm in filled pressure). In the high angle region (150° and 90°) the detectors are located at geometrical time focusing positions, while in the lower angle region they are located at electrical hardware time focusing positions described later in detail. The scattered flight path length has been determined to give both high

count rates and modest geometrical Q resolution. The scattering angle and the flight path length for each detector now used are listed in Table 1.

The electrical hardware time focusing system which consists of a CAMAC module was newly developed.<sup>2)</sup> The block diagram is shown in Fig. 2. The new system is the same in principle as the time focusing one using a computer. The main difference between the two systems is that the former system does not need any computing time so that it can fit measurements with the higher count rate. In this system each detector has own time analyser, of which the time width  $\Delta\tau$  is chosen easily by a software to satisfy the following time focusing condition.

$$\Delta\tau = \frac{L \sin\theta}{L_r \sin\theta_r} \Delta\tau_r, \quad (1)$$

where L and  $2\theta$  are the total flight path length and the scattering angle, respectively. Subscript r denotes the reference detector. The all time analysers (sub modules in Fig. 2) involved in a certain detector bank are controlled by one main module. The counts accumulated in a sub module during time interval  $\Delta\tau$  are added to the stored counts in the corresponding address in Q-space of the main memory giving a time-focused result. The system is controlled by a personal computer PC 9800 (NEC). Acceptable maximum count rate is expected to be about 6 counts/ $\mu$ s per each time analyser.

### 3. Geometrical resolution

The resolution in Q space was estimated by a Monte Carlo technique. The geometrical sizes of moderator ( $100 \times 100 \text{ mm}^2$ ), sample (8 mm in diameter and 40 mm in height as a typical case) and detector (1/2" in diameter and 4 ~ 12" in length depending on scattering angles) were taken into account. The time structure of the incident neutron pulse was included in an approximate manner as well. The resolution  $\Delta Q$  was defined as a root mean square deviation of the Q value from the mean value  $\bar{Q}$ , i.e.  $\Delta Q = \langle (Q - \bar{Q})^2 \rangle^{1/2}$ . The calculated results are shown in Fig. 3. The broken lines show the case of the poor resolution, while the solid lines do the case of the good resolution. In the latter a limited detector height was assumed except for 90° detectors, while in the former a slightly off time focusing position was chosen for 90° detector bank.

Usually we utilize the neutrons only in the wavelength range of 0.3 - 0.7 Å for the S(Q) measurement, except for the low Q measurement with low angle counter, in order to avoid the serious distortion of S(Q) arising from non-constant Q scan of the instrument. The range between the two dots on each curve in the figure corresponds to this wavelength range. Figure 4 demonstrates the effect of the geometrical resolution on the simulated S(Q) for a model system. The result suggests that the resolution  $\Delta Q$  must be at least  $0.2 \text{ \AA}^{-1}$  or less if one requires the precise measurement of S(Q).

#### 4. Effect of the inelastic scattering

The inelastic scattering is a serious problem in the S(Q) measurement when a sample contains light atoms. In order to know how the inelastic scattering affects observed S(Q) at high Q, we simulated experiment on the HIT using the following simple models of S(Q,ω)'s.

$$\begin{aligned}
 S_{\text{self}}(Q, \omega) &= \left[ \frac{M}{2\pi\hbar^2 Q^2 kT} \right]^{1/2} \exp \left[ - \frac{M}{2\hbar^2 Q^2 kT} \left( \hbar\omega - \frac{\hbar^2 Q^2}{2M} \right)^2 \right], \\
 S_{\text{int}}(Q, \omega) &= \left[ \frac{M^*}{2\pi\hbar^2 Q^2 kT} \right]^{1/2} \exp \left[ - \frac{M^*}{2\hbar^2 Q^2 kT} \left( \hbar\omega - \frac{\hbar^2 Q^2}{2M^*} \right)^2 \right] \\
 &\cdot (S(Q)-1), \tag{2}
 \end{aligned}$$

where M is the atomic mass and  $M^*$  is the effective mass for the coherent scattering just for convenience. This model is enough to examine the effect of the inelastic scattering on S(Q) in high Q region although it is not in low Q. In the simulation an incident neutron spectrum  $\Phi(E)$  was approximated by the following analytical form,

$$\Phi(E) = \Phi_0 \left[ \Phi_{\text{th}} \left( \frac{E}{E_T} \right) \exp \left( - \frac{E}{E_T} \right) + \Phi_{\text{epi}} \frac{\Delta(E)}{E^{0.878}} \right], \tag{3}$$

where  $E_T = 35.2 \text{ meV}$ ,  $\Phi_{\text{th}}/\Phi_{\text{epi}} = 6.89$  and  $\Delta(E) = 1/[1 + (5E_T/E)^7]$ .

The detector efficiency  $\eta(\lambda)$  was approximated by the following equation,

$$\eta(\lambda) = 1 - \exp(a + b\lambda + c\lambda^2) \quad (0.05 < \lambda < 9.6 \text{ \AA}), \quad (4)$$

where  $a = 0.01839$ ,  $b = -1.44457$  and  $c = 0.007479$ . Figure 5 shows the instrumental integration paths calculated for the HIT machine. The integration of  $S(Q, \omega)$  with respect to  $\omega$  is carried out by the HIT along these integration paths with weighted factors of  $\Phi(E)$  and  $\eta(\lambda)$ .  $S(Q)$ 's simulated for  $M/m = 100$  and  $M^*/m = 200$ , where  $m$  is a neutron mass, are shown in Fig. 6. The effect of the inelastic scattering on the simulated  $S(Q)$  is not serious as expected for samples with heavy mass. On the other hand for samples with light mass such as  $M/m = 11$  and  $M^*/m = 27$  the effect is serious as shown in Fig. 7. The following three effects on the  $S(Q)$  due to inelastic scattering may be confirmed :

- i) deviation of  $S_{\text{self}}(Q)$  from the unity,
- ii) damping of the oscillation of  $S(Q)$ , and
- iii) phase shift of the oscillation of  $S(Q)$ .

All of three effects are significant at higher scattering angle. We have often encountered these three effects in actual experiments. Among these three effects, the second and the third are very important for structural investigations.

Powles<sup>3)</sup> proposed a correction method for the inelastic scattering for various molecules, but it seems hard to make precise corrections when a sample contains three or more chemical species. The materials we are interested in are often multi-component systems, such as aqueous solutions. Therefore, we are planning to install a new detector systems at the lower scattering angles (less than  $30^\circ$ ) using  $^6\text{Li}$  glass scintillators. In order to measure the  $S(Q)$  in the range of  $Q$  over  $30 \text{ \AA}^{-1}$  or more with a reasonable resolution, the momentum resolution must be less than  $0.2 \text{ \AA}^{-1}$  in the whole  $Q$  range. To achieve this required resolution and to still keep good count rate, a coarse converging collimator may be useful, and the glass scintillators will be arranged as many as possible along the Debye-Scherrer cone on a focusing sphere of the converging collimator. Design work to improve the HIT is in progress.

#### Acknowledgement

The authors would thank Mr. S. Satoh for providing the new time analyser system including computer software. Their thanks are also to all members of the HIT group.

## References

- 1) N. Watanabe, T. Fukunaga, T. Shinohe, K. Yamada and T. Mizoguchi, Proc. of ICANS-IV, KENS Report II (1981), 539.
- 2) S. Satoh, KEK Internal 85-8 (1985) (in Japanese).
- 3) J. G. Powles, Molec. Phys. 36 (1978), *ibid* 37 (1979) 623.

Table 1. Parameters of the HIT machine

( Scattered flight path length at detector center  $L_2$ , scattering angle at detector center  $2\theta$  and time width of time analyser  $\Delta t$ )

Detectors	$L_2$ (mm)	$2\theta$ (degree)	$\Delta t$ ( $\mu$ sec)	Note
<u>150° bank</u>				
150 a2	301.6	155.3	2.0	geometrical time focusing
150 a3	327.0	152.5		
150 a4	349.9	150.0		
<u>90° bank</u>				
90 a1	255.5	93.6	2.0	geometrical time focusing
90 a2	330.0	90.2		
90 a3	418.3	87.6		
<u>50° bank</u>				
50 b1	514.1	42.0	4.0	electrical hardware time focusing
50 b4	500.5	47.8	4.5	
<u>30° bank</u>				
Fa 15	586.3	26.2	4.0	electrical hardware time focusing
Fa 18	557.0	31.5	4.75	
<u>20° bank</u>				
Fa 11	631.1	20.0	8.0	electrical hardware time focusing
Fa 13	607.17	23.0	9.125	
<u>13°</u>				
Fa 6	697.6	13.3	8.0	
<u>7°</u>				
Fa 6	779.4	7.4	8.0	

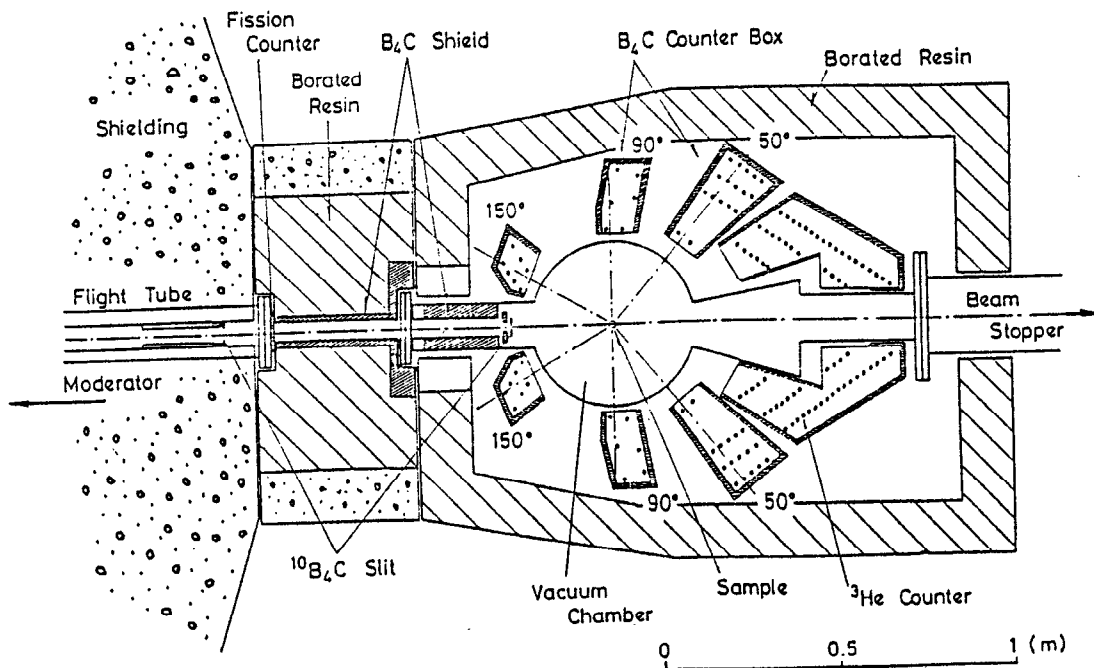


Fig. 1. A schematic drawing of the current HIT machine.

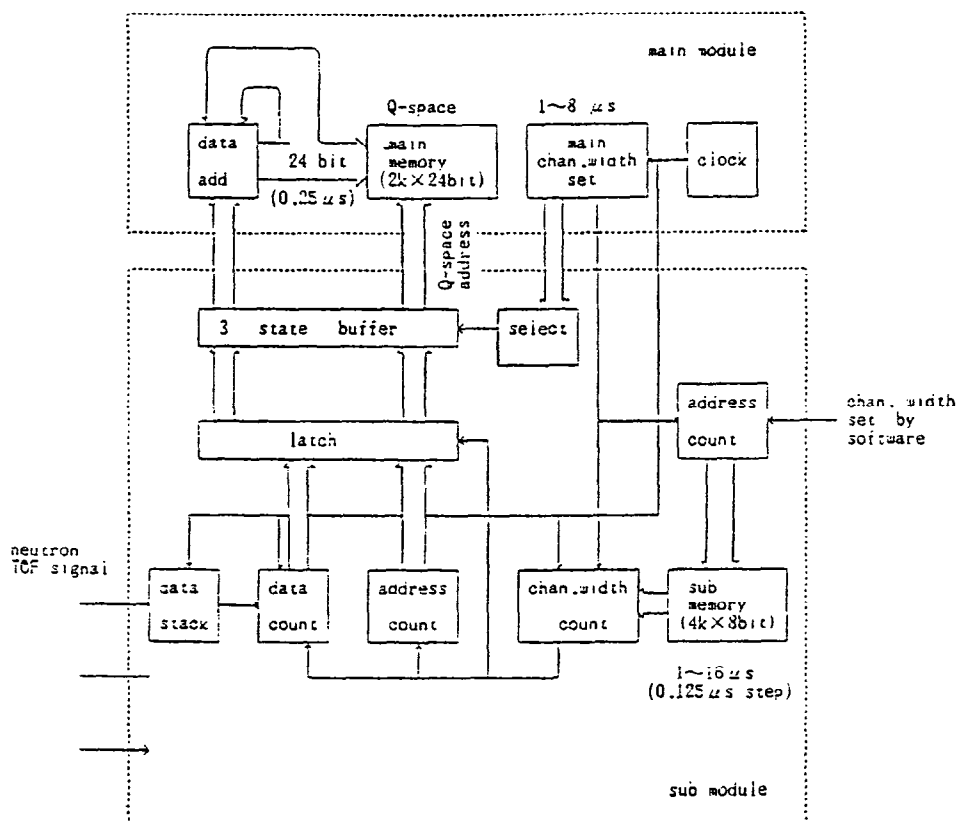


Fig. 2. Block diagram of CAMAC module for hardware time focusing.

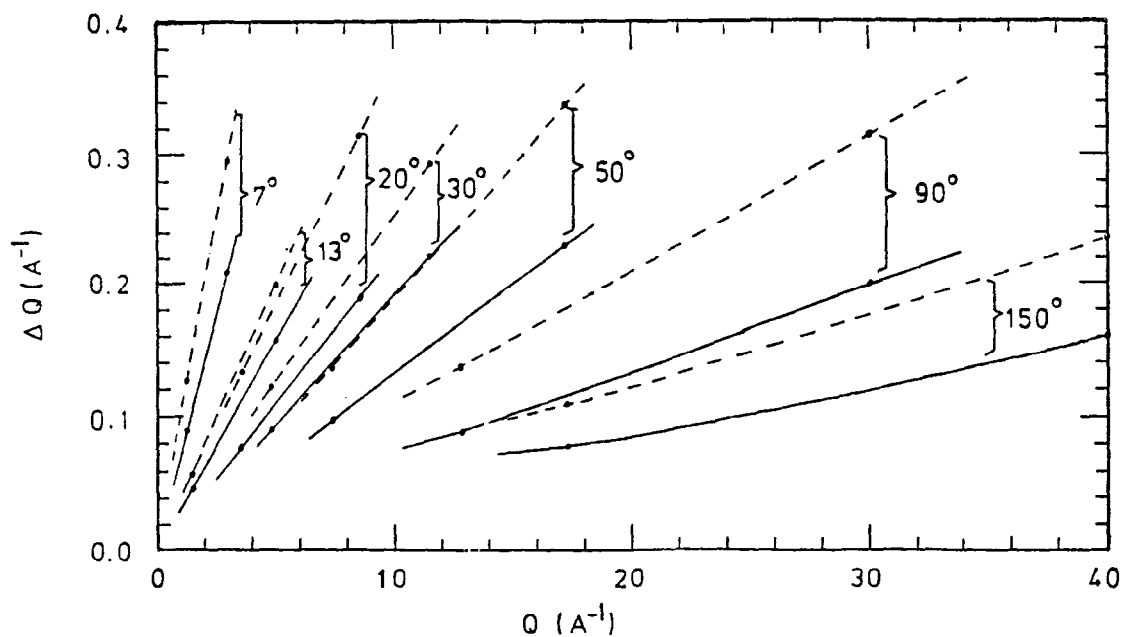


Fig. 3. Geometrical resolution of momentum transfer  $Q$  calculated for various detector banks now used in the HIT. Broken lines show poor resolution, while solid lines good resolution. The region between two dots on each line corresponds to the wavelength between 0.3 and 0.7 Å.



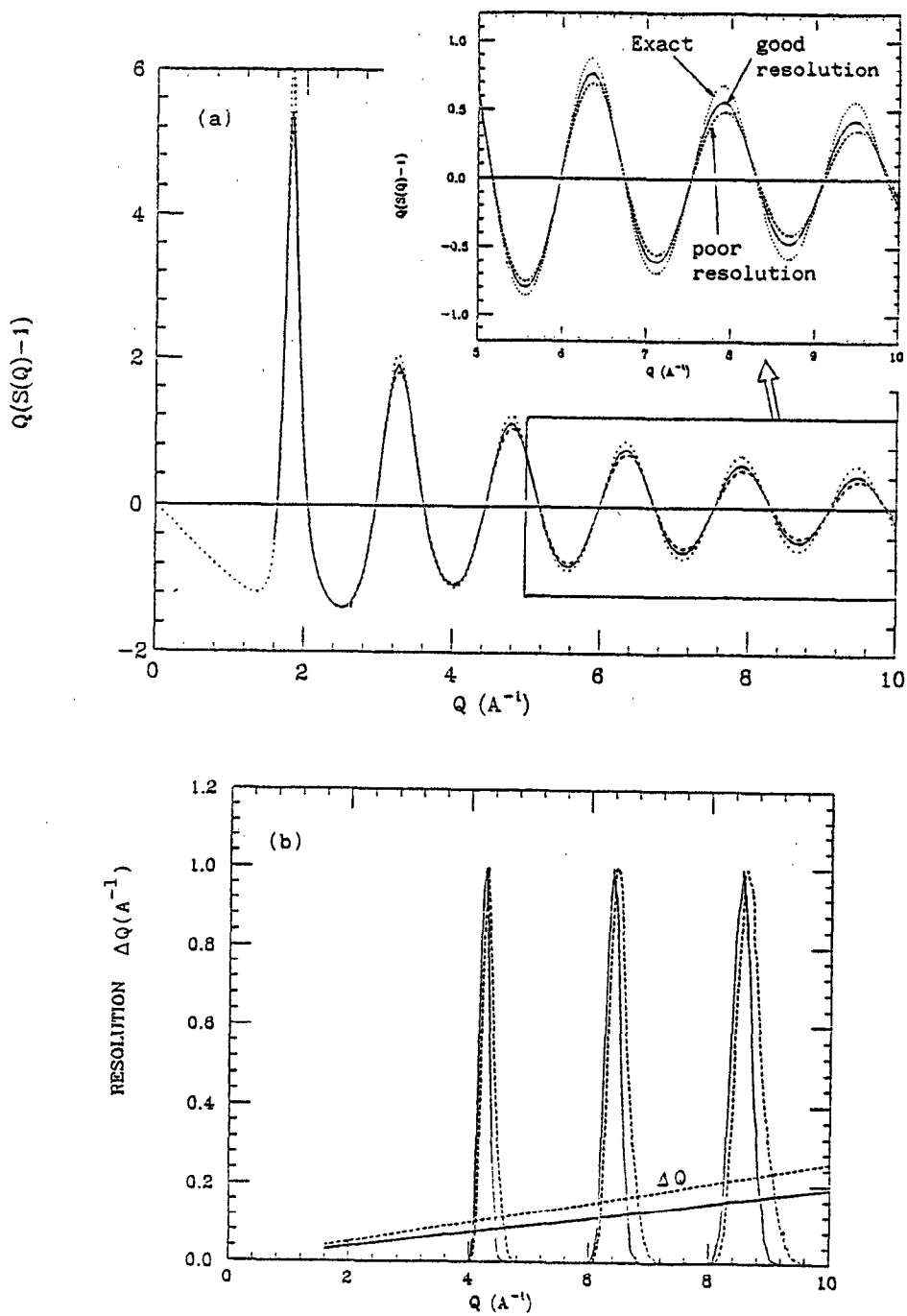


Fig. 4. Effect of the  $Q$  resolution on  $S(Q)$ .

(a) The dotted curve is an exact  $S(Q)$  calculated for hard sphere system. Broken and solid curves are the  $S(Q)$ 's calculated with the poor and good resolutions shown in the lower figure.

(b) A resolution  $\Delta Q$  for  $2\theta = 30^\circ$  which is the same as already shown in Fig. 3. Solid line shows good resolution, while broken line poor resolution. Resolution functions at ca.  $4.2, 6.4$  and  $8.5 \text{ \AA}^{-1}$  are shown as well.

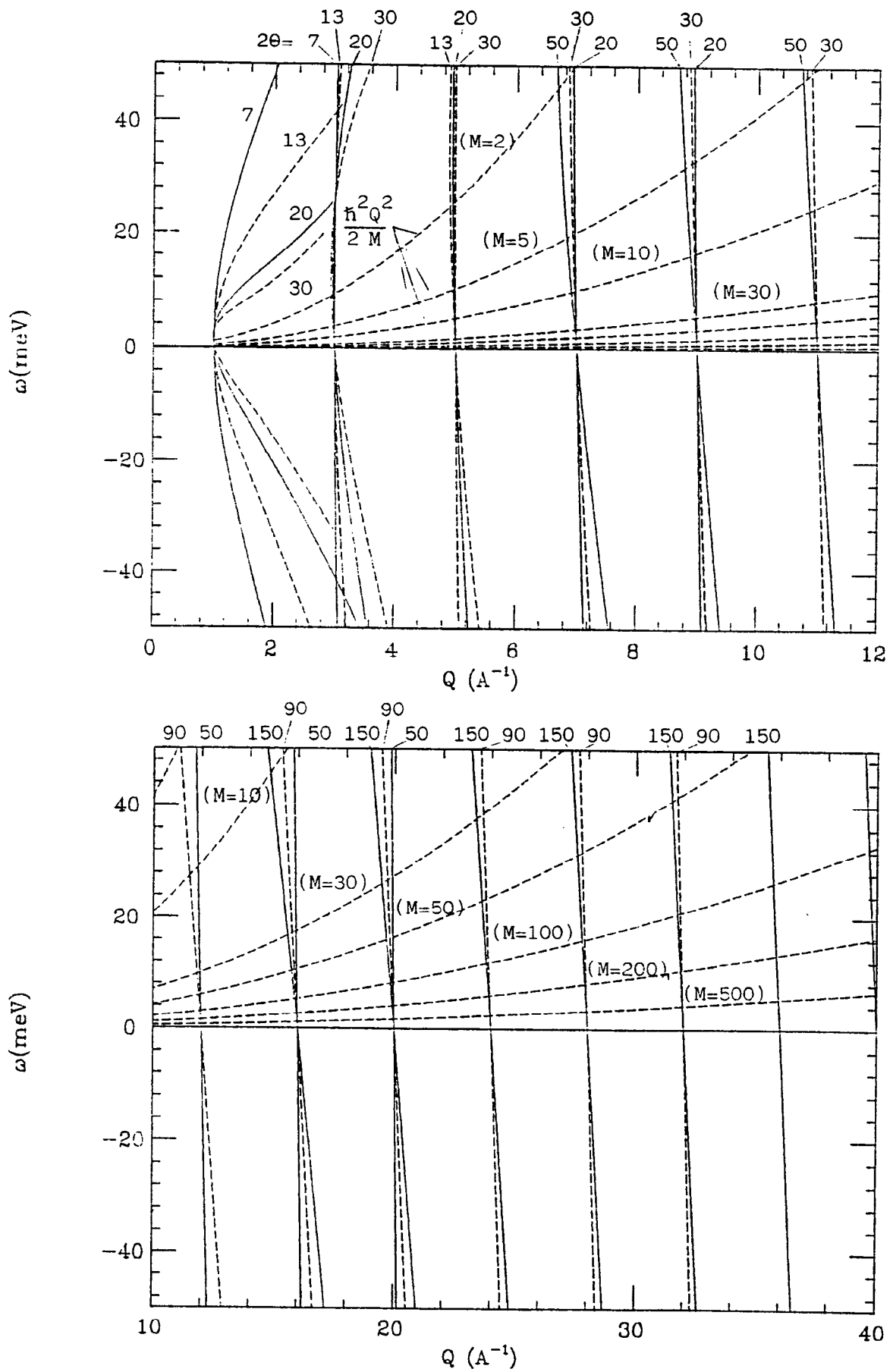


Fig. 5. Instrumental integration paths of the HIT. Curves of recoil energy  $\hbar^2 Q^2 / 2M$  for various  $M$ 's are also shown.

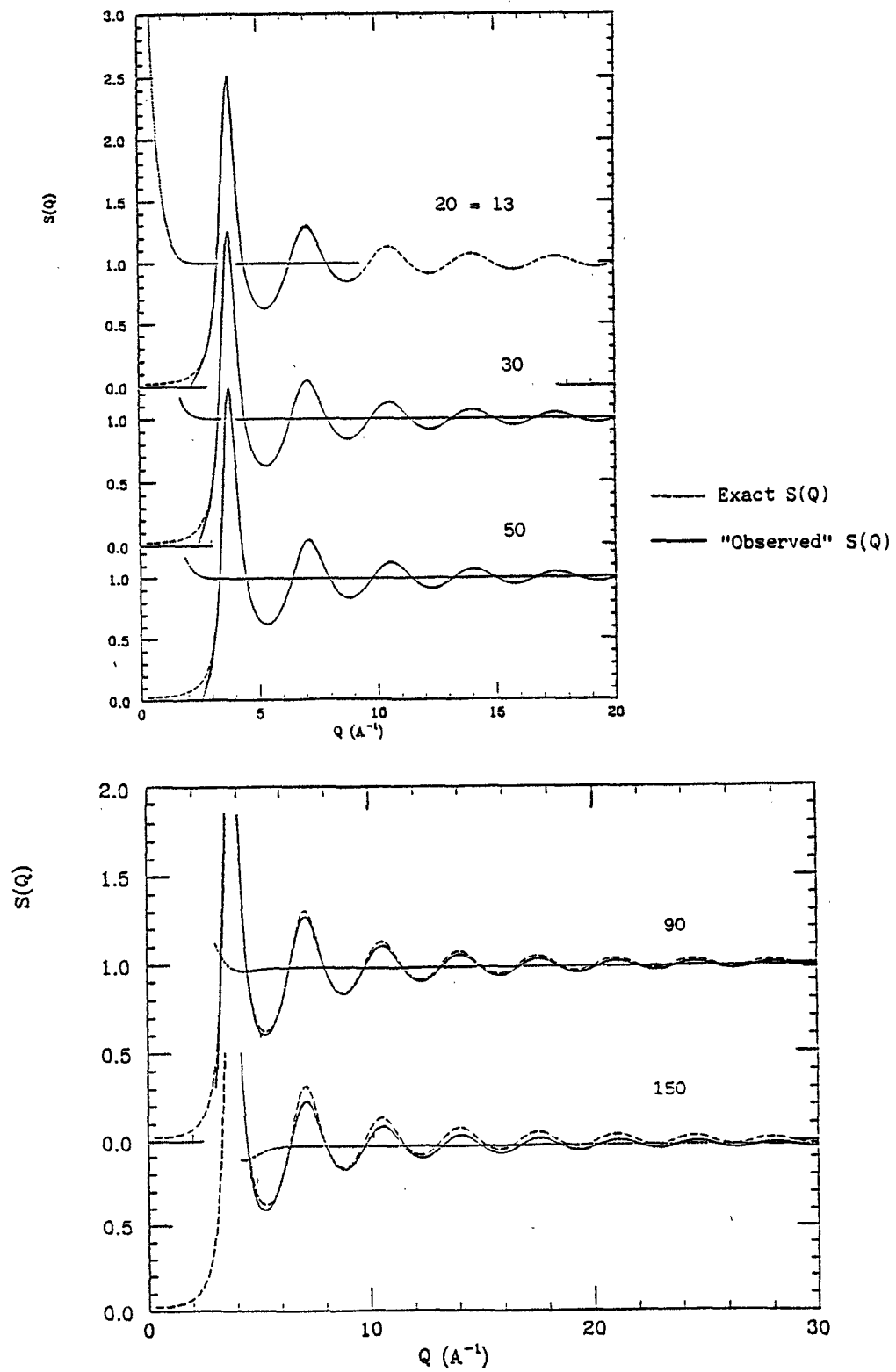


Fig. 6. The comparison of  $S(Q)$ 's simulated for heavy nuclei ( $M/m = 100$ ,  $M^*/m = 200$ , solid curves) and exact ones (broken curves).

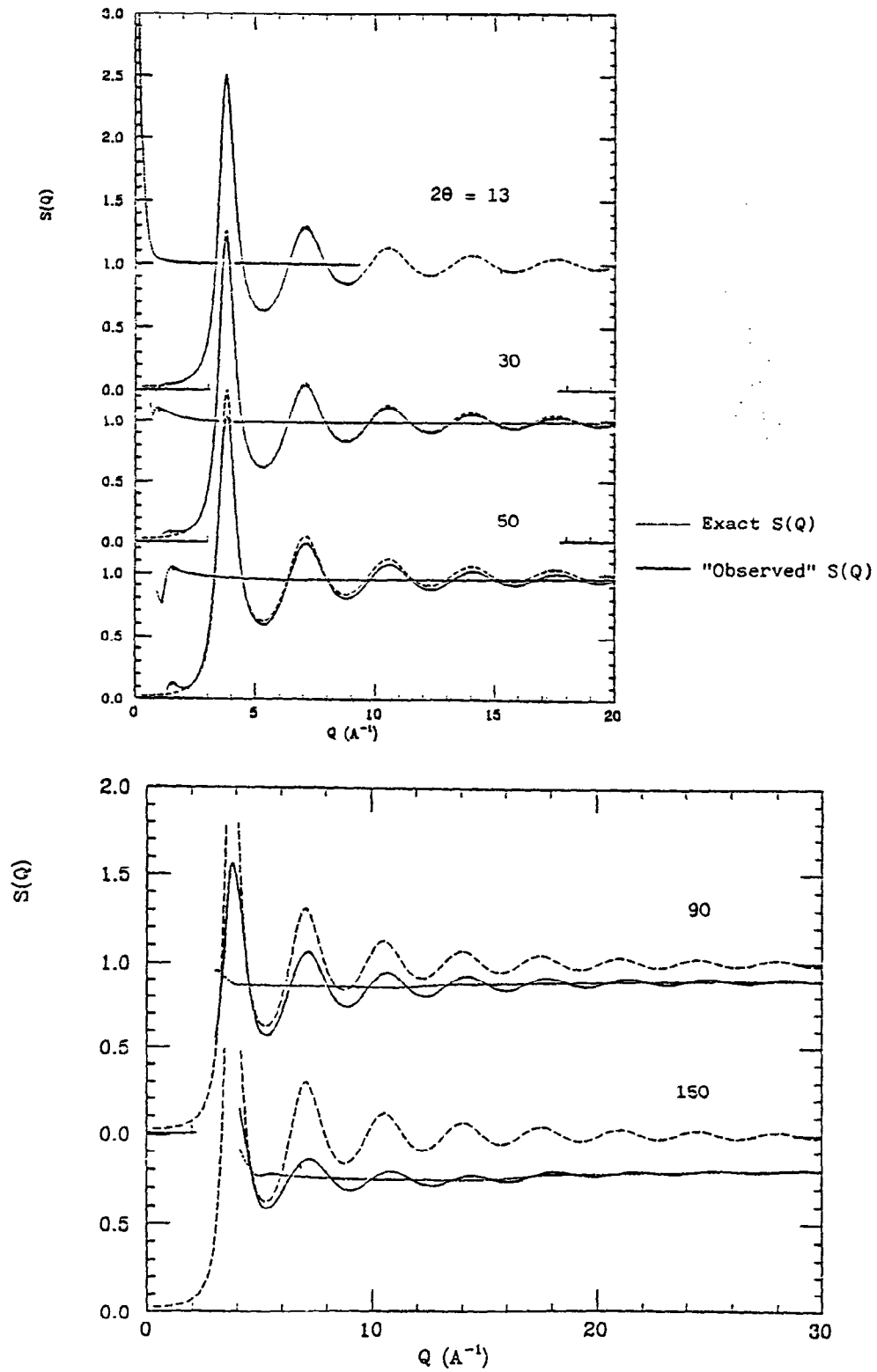


Fig. 7. The comparison of  $S(Q)$ 's simulated for light nuclei ( $M/m = 11$ ,  $M^*/m = 27$ , solid curves) and exact ones (broken curves).